A particle tracking velocimetry technique for drop characterization in agricultural sprinklers

C. Bautista-Capetillo, O. Robles, H. Salinas & E. Playán

Irrigation Science

ISSN 0342-7188

Irrig Sci
DOI 10.1007/s00271-014-0440-6

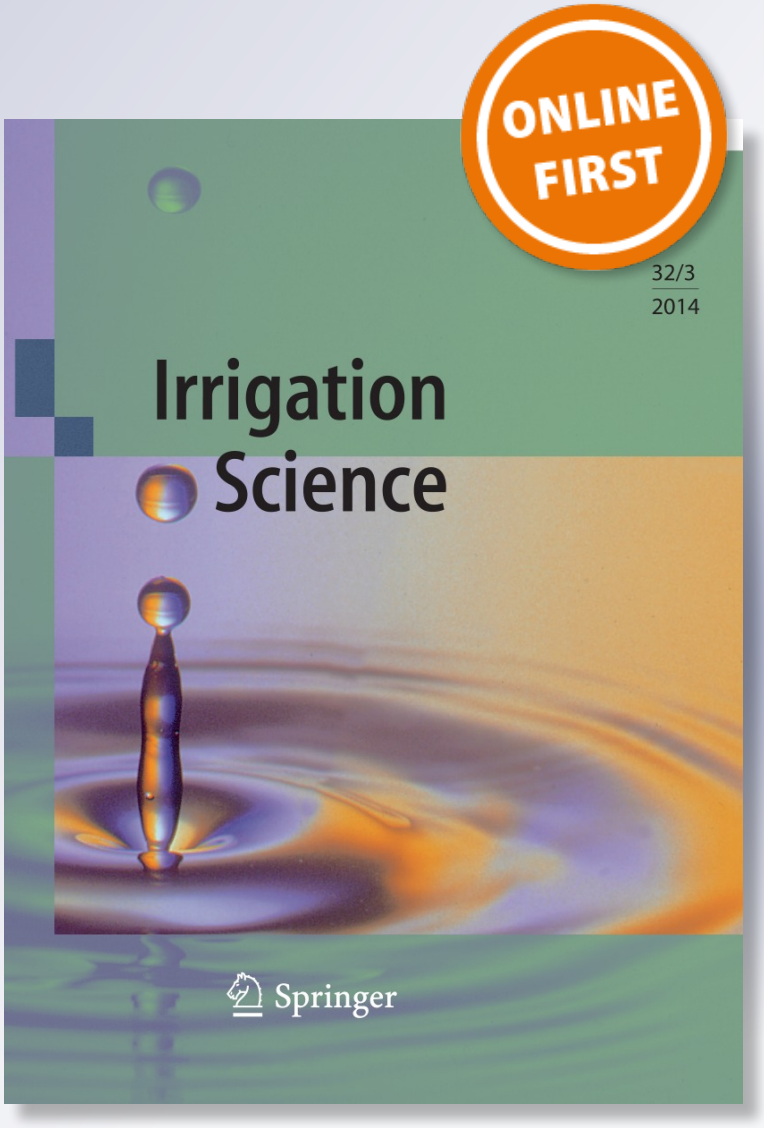

Springer

Irrig Sci
DOI 10.1007/s00271-014-0440-6

ORIGINAL PAPER

A particle tracking velocimetry technique for drop characterization in agricultural sprinklers

C. Bautista-Capetillo · O. Robles · H. Salinas · E. Playán

Received: 22 October 2013 / Accepted: 22 May 2014

Abstract A variety of techniques have been proposed in the literature for sprinkler drop characterization. An optical particle tracking velocimetry (PTV) technique is proposed in this paper to determine drop velocity, diameter and angle. The technique has been applied to the drops emitted by an isolated impact sprinkler equipped with two nozzles (diameters 3.20 and 4.37 mm) operating at a pressure of 175 kPa. PTV has been previously used to determine the velocity vector of different types of particles. In this research, PTV was used to photograph sprinkler drops over a region illuminated with laser light. Photographs were taken at four horizontal distances from the sprinkler, which was located at an elevation of 1.65 m over the soil surface. Drop angle and velocity were derived from the displacement of the drop centroid in two images separated by a short time step. Centrality and dispersion parameters were obtained for each drop variable and observation point. Results derive from the analysis of 2,360 images. Only 37.5 % of them (884 images) contained drops which could be processed by the PTV algorithm, resulting in a total of 3,782 drops. A filtering algorithm just validated 1,893 valid drops, which were successfully analyzed. The proposed technique uses expensive equipment requiring continued protection against irrigation water. This methodology has proven valuable to characterize irrigation water drops. Despite its robust measurement procedure, further comparison with other techniques seems necessary before this optical technique can be recommended for practical use in sprinkler drop characterization.

Communicated by J. Li.

C. Bautista-Capetillo (✉) · O. Robles
Maestría en Ingeniería Aplicada Orientación Recursos Hidráulicos, Universidad Autónoma de Zacatecas, Avda. Ramón López Velarde, 801, Zacatecas, Zacatecas, Mexico
e-mail: baucap@uaz.edu.mx

H. Salinas
Centro Interamericano de Recursos del Agua, Universidad Autónoma del Estado de México, Carr. Toluca-Ixtlahuaca km. 14.5 San Cayetano de Morelos, Toluca, Estado de México, Mexico

E. Playán
Departamento Suelo y Agua, Estación Experimental de Aula Dei, CSIC, P. O. Box 13034, 50080 Saragossa, Spain

Introduction

A sprinkler irrigation system distributes water in the form of discrete drops traveling through the air (Kincaid et al. 1996). Each drop typically reaches a different horizontal distance from the sprinkler, depending on its initial velocity vector (module and vertical angle) and diameter. The statistical distribution of these variables in the population of drops emitted by a sprinkler is subjected to several factors: the type of sprinkler and nozzle, the operational hydraulic parameters and the environmental conditions (Bautista et al. 2009).

Experimental drop characterization is an important subject for purposes related to irrigation management. One of them is the assessment of Wind Drift and Evaporation Losses (WDEL) (Tarjuelo et al. 2000). These losses are commonly estimated from the difference between the amount of water discharged by the sprinkler and the amount of water collected at catch cans distributed along the field. WDEL directly depend on climatic and operational conditions (Bavi et al. 2009), including drop diameter. Additionally, a number of papers have focused on the effect of drops' impact on soil properties (Seginer 1965; Kohl et al. 1985; Thompson and James 1985; Kincaid

Published online: 07 June 2014

1996; Basahi et al. 1998; Bautista et al. 2012). The kinetic energy contained in large, fast-moving drops is transferred to the soil surface upon landing, potentially causing crusting, runoff and erosion. As a consequence, the soil infiltration rate can be severely reduced (Kohl 1974; Montero et al. 2003). Finally, the numerical simulation of sprinkler irrigation through ballistic theory requires characterization of drop diameter (Seginer 1965; Fukui et al. 1980).

Numerous methodologies have been applied to the characterization of sprinkler drops such as stain method, oil immersion method, momentum method, photograph method or optical methods. These techniques were used for precipitation studies (Wiesner 1895; Jones 1956; Pearson and Martin 1957; Kunkel 1971; Beard 1976; Hauser et al. 1984; Jadhav 1985; Eigel and Moore 1983; Ulbrich 1983; Sheppard 1990; Salles et al. 1999). Some of these methods were later implemented to evaluate sprinkler irrigation. This is the case of Kohl and DeBoer (1984), who implemented the flour method. In this method, drops impacting on a thin flour layer create pellets whose mass is related to drop diameter. Sudheer and Panda (2000) proposed a technique based on image processing to obtain drop size measurements using a high-resolution and high-speed camera. Montero et al. (2003) measured the attenuation of a luminous beam using an optical disdrometer. Recently, Salvador et al. (2009) used a low-speed photographic method to characterize drops at different horizontal distances from an impact sprinkler.

At the end of the twentieth century, several techniques were developed to measure flow motion under different hydraulic conditions. These techniques include the following: laser Doppler anemometry (LDA), hot-wire anemometry (HWA), laser-induced fluorescence (LIF), Doppler global velocimetry (DGV) and Doppler phase anemometry (PDA). Due to the emergence of high-speed cameras and sophisticated laser equipment, noninvasive techniques have been proposed to evaluate flow properties through computational visualization methodologies such as particle image velocimetry (PIV) and particle tracking velocimetry (PTV) for two-dimensional flow analysis, as well as Stereo-PIV technique (S-PIV) and digital holography for three-dimensional flow analysis (Adrian 1991; Jensen 2004). These techniques provide highly efficient tools to characterize patterns in velocity, temperature, pressure, stress–strain, vibration, turbulence and vorticity in flows of different nature (Van Dyke 1982; Smits and Lim 2000). These techniques also permit to process thousands of data in relatively short times.

The characterization of isolated drops has recently been attempted using low-speed photographic techniques (Bautista et al. 2009; Salvador et al. 2009). Critical disadvantages of this methodology include the following: (a) The number of pictures should be large, since a considerable percentage of pictures are discarded due to lack of reliable information; the decision to include or remove an image depends on the criterion of the analyst; (b) drop variables required to estimate diameter, velocity and angle are manually measured, causing perception errors; and (c) the characterization of one drop requires between 4 and 7 min.

Optical techniques, such as PIV or PTV have been recently applied to the characterization of spherical and non-spherical sedimentary particles moving at low speeds (<95 cm s^{-1}) and analyzed as a two-phase flow (particle and fluid velocity are independently determined) (Salinas et al. 2006; Salinas and García 2011). The PTV technique bases its operation on high-speed image acquisition and high-spatial resolution. This technique can obtain and analyze an image in 2–5 ms, a factor which constitutes a critical competitive advantage. Moreover, the technique can be applied to obtain 2D velocity vector maps at any specific time. Velocity vectors are determined from individual drop displacement during a certain amount of time (Adrian 1991; Prasad 2000; Jensen 2004). When PTV was applied to the characterization of sedimentary particles, a CCD camera focused on a flow region seeded with tracer particles (with density similar to the fluid). The region was illuminated with a laser light sheet to have tracer particles reflect light, which was captured by the CCD camera. When the system is programmed to produce double-pulsed laser sheets, each light pulse perceives the same particle at different times and locations. As a consequence, the same tracer element appears twice in one image. Subsequently, digital image processing is used to measure the distance between the centroids of double-pulsed drops. The combination of this distance and the time between both light pulses is used to determine the particle velocity vector (Prasad 2000; Salinas et al. 2006). This technique has been mainly used to characterize sedimentation velocity in non-cohesive particles (i.e., sand) (Salinas and García 2011). However, some authors have suggested the possibility of applying it to the characterization of drops emitted by flow-pulverizing devices, cavitating or solid particles in mixed tanks (Sang and Yu 2004; Salinas et al. 2006).

This paper reports on the application of a PTV technique to the characterization of the drops emitted by an irrigation sprinkler in the absence of wind (indoor conditions). The specific goals of this study were as follows: (1) to characterize drop diameter, velocity and angle at different horizontal distances from the sprinkler; and (2) to test the adequacy of a PTV algorithm developed by Salinas et al. (2006) to obtain 2D velocity fields.

Materials and methods

The PTV system

The PTV system used in this research was composed by five elements: (1) a high-speed CCD camera manufactured

by Lumenera Co. model LU175, with a temporal resolution of 60 frames per second and a spatial resolution of 640 by 480 pixels, equipped with a 50 mm lens manufactured by Nikkor and located at an elevation of 1.65 m over the soil surface; (2) a 15 mJ double-pulsed laser type Nd:YAG, manufactured by New Wave; (3) a set of optical accessories (mirrors and lenses); 4) a synchronizer (trigger) to control the image acquisition sequence and the laser light; and 5) the PTV-SED version 1.0 software for image processing, developed in MATLAB by Salinas et al. (2006).

Validation of PTV drop diameter measurements

Two experiments were performed to validate PTV drop diameter measurements. Before each test, calibration images were obtained by placing a reference ruler at the picture background to determine the image scale (pixels/cm). First, PTV was used to obtain the diameter of polyamide particles with real diameters of 25.0 and 50.0 μm (values provided by the manufacturer), a density of 1.03 g/cm^3, and seeded on a channel with water flow velocities of 0.05–0.90 m/s. Second, spherical steel pellets with real diameters of 3.80, 4.20 and 6.42 mm (as measured with a vernier caliper) were analyzed. Particles rolled down a plate with obstacles, resulting in a hazardous motion. The plate was kept at different slopes (10°, 20° y 30°) relative the horizontal plane in order to generate different motion patterns. Photographs were taken at 1.5 m from the nails plate, and the camera was re-positioned at each change of slope so that both elements remained parallel. Images were captured every 0.04 ms for each run over the analysis region (including the plate and a reference ruler). The camera was manually focused to the reference ruler. In both experiments, diameter validation consisted in comparisons between real diameter and PTV diameter (using the PTV-SED version 1.0 software).

The sprinkler irrigation experimental setup

This research was carried out at the facilities of Centro Interamericano de Recursos del Agua (CIRA), depending on the Universidad Autónoma del Estado de México (Toluca, México). The experimental setup is schematically presented in Fig. 1, which is composed of two parts: the irrigation system and the PTV system. The irrigation system was composed by: (1) a water tank with a capacity of 0.8 m^3; (2) a hydro-pneumatic pump manufactured by Myers, with a power of 0.37 kW and equipped with a pressure regulating tank and a 600 kPa ABS radial manometer manufactured by Fimet; (3) an isolated sprinkler manufactured by WadeRain, model WR-33, with two nozzles (3.20 and 4.37 mm) located at an elevation of 1.8 m over the soil surface, with a nozzle angle respect to the horizontal of 27°; and (4) a 20 mm in diameter PVC pipe.

Determination of the sprinkler radial application pattern

In order to characterize the sprinkler, the ISO 15886-3 standard (Anonymous 2004) was applied to the design of the experiment required to characterize the sprinkler radial application pattern. Pluviometers were cylindrical in shape, had a diameter of 0.16 m and were spaced at 0.60 m intervals, to a distance of 13 m. Nozzle pressure was set to 175 kPa. The experiment lasted for 60 min. Water and air temperature was 10 °C. Before performing the experiments, the sprinkler was run for a few minutes in order to standardize environmental conditions.

Drop characterization: experimental procedures

A radial line was marked on the soil, extending from the sprinkler to the last observation point. Four observation points were arranged at horizontal distances from the sprinkler of 5, 7, 9 and 12 m. Drops emitted by the main and secondary jets were analyzed together at distances of 5 and 7 m; at further distances, only drops resulting from the main jet were present. When using the PTV technique, it is common to use tracers to visualize the fluid behavior. Due to the nature of this experiment, it was not possible to employ them. In fact, the illuminated drops needed to diffract light to be captured by CCD sensor. Consequently, tests were performed in complete darkness, and the capture zone was illuminated with a laser source. This setup permitted to obtain images containing perceptible information for digital processing (Salinas et al. 2006).

The light beam was directed to the capture zone using optical mirrors located at a 45° angle, as presented in Fig. 1. Once the beam light was in the capture zone, it was amplified using optical lenses to obtain a larger sheet than the area covered by the camera lens (60 by 50 mm). The distance separating the CCD device lens and the laser sheet was 1.0 m in all cases. Further, the laser beam thickness was adjusted to 3.0 mm to guaranty that characterized drops were on the same analysis plane. The technique requires synchronization between laser pulses and the opening/closing of the camera shutter. The CCD camera and the trigger were computer-operated following a programmed time sequence. Several preliminary tests were performed to establish the optimum time between laser pulses (Δt). Optimum Δt permits to appreciate the position of a given drop at two different times within the same image. Similarly, the exposure time (t_{exp}) was optimized to maximize the number of detected drops. Optimum values for all captures were $\Delta t = 2.0$ and $t_{exp} = 20$ ms, as presented in Fig. 2. These times led to sharp drop images

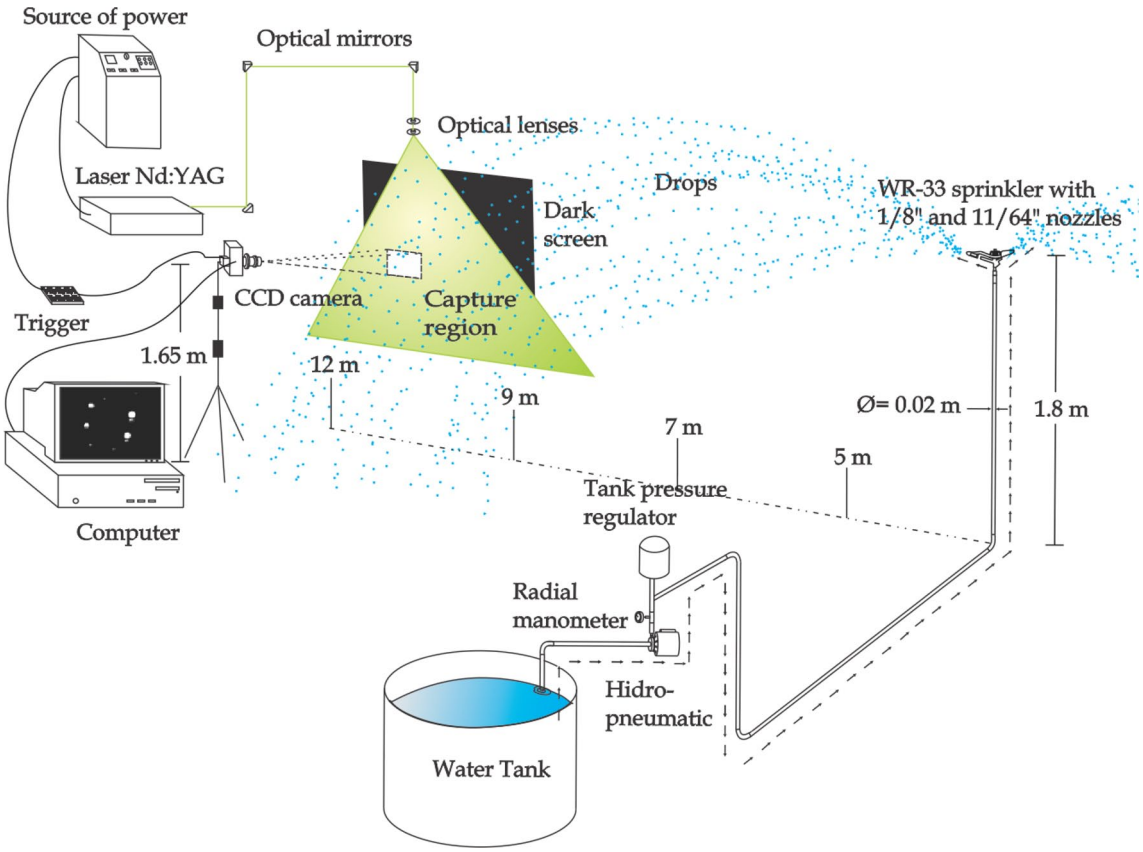

Fig. 1 Experimental setup for drop characterization using the PTV technique. The figure presents the PTV system (computer, laser, synchronizer, optical equipment, CCD camera and observation points) and the isolated sprinkler irrigation system (water tank, hydro-pneumatic pump, manometer, tank pressure regulator, PVC pipe 0.02 m diameter and sprinkler with double nozzle)

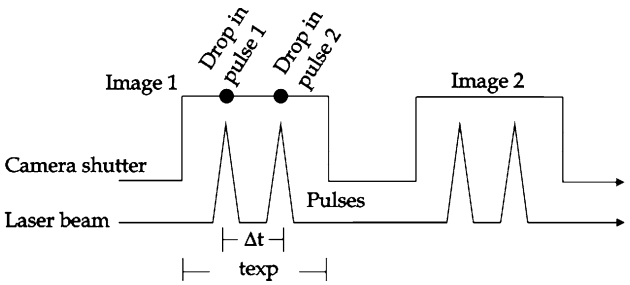

Fig. 2 Synchronization between the camera shutter and the laser beam to perform double-capture of sprinkler irrigation drops

and permitted to determine their diameter, displacement and ultimately their velocity. When the sprinkler jet approached the measurement line, the camera shooting and laser devices were activated in continuous mode. Shooting stopped when drops could no longer be appreciated. Drop density was very high in images shot near the sprinkler, while at the distal areas a large number of photographs were required to obtain a representative sample of the local drop population.

The PTV-SED software version 1.0, originally developed to analyze the fall velocity of sedimentary particles in two-phase flows (Salinas et al. 2006), was used to characterize sprinkler drops. The algorithm was modified to accommodate the difference between sprinkler drop geometry and sediment geometry. PTV operation comprises two sequential procedures. The first procedure implies improving image quality through spatial filtering. In this procedure, image noise is eliminated to ensure that detected particles are clearly visible. The second procedure implies detecting drops in each pulse following five processes (Salinas et al. 2006): (1) identify maximum and minimum intensity over the monochromatic image (black or white) to determine droplet size making a search to indicate the change between these two intensities.; (2) from drop geometry evaluated from pixel intensity, a circular surface is formed identifying drop boundaries and determining the cross-sectional drop area (A), determine drop diameter from $D = 2 * \sqrt{A/\pi}$; (3) obtain the coordinates (x, y) of the drop centroid (making use of pixel intensity); (4) identify pairs of double-pulsed droplets;

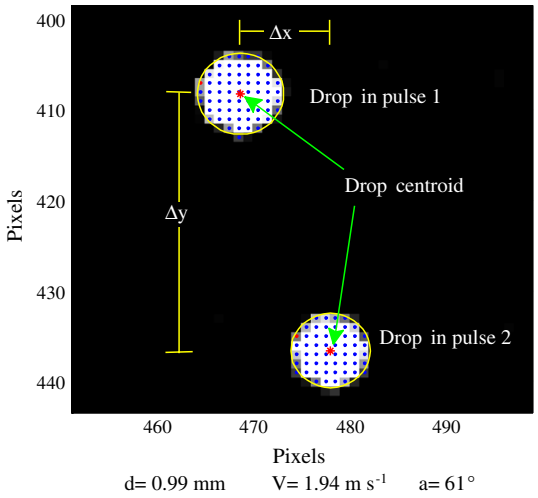

Fig. 3 Drop captured at two different times (t, $t + \Delta t$). The horizontal (Δx) and vertical (Δy) displacement of the drop centroid at each pulse is presented, along with the estimation of drop diameter from pixel intensity. In the figure, d = drop diameter; V = drop velocity; and a = drop angle

determine the distance separating their centroids (Δx, Δy); and (5) obtain the velocity vector (u, v) using the following equation:

$$u = \frac{\Delta x}{\Delta t} \quad v = \frac{\Delta y}{\Delta t} \tag{1}$$

Initial software parameters were set for each location of the PTV system. The image scale was obtained from the internal calibration provided by the reference ruler installed in the analysis region. Values of 110, 105, 103 and 105 px cm^{-1} were determined for distances of 5, 7, 9 and 12 m from the impact sprinkler, respectively. Maximum and minimum intensity thresholds depend on the amount of noise present in the images and on the light reflected by the drops. The PTV system registers intensity in a 0–255 range (Salinas et al. 2006). In order to progress toward drop identification, 25 images per capture point were visualized to characterize the distances and angles separating doubled-pulsed drops. Space ranges of 5–20, 5–30, 10–40 and 15–80 px were found at each capture distance, giving a first estimate of drop velocity variability. Moreover, the interval of drop angle variability was defined as 245°–360°. Figure 3 presents a sample double-pulsed drop image. In this figure, the horizontal and vertical distances separating the centroids are presented, together with the circumference used to estimate drop diameter.

Despite the short time separating both laser pulses, in some cases, a given drop was not adequately depicted in the second pulse. In these cases, the drop moved outside the analysis plane (due to a velocity component perpendicular to it). Consequently, drop diameter and the location of the centroid could not be adequately determined in the second pulse. In order to control this problem, algorithms were programmed to reject drops showing 20 % difference between diameters 1 and 2. This procedure discarded almost 50 % of the drops. The remaining drop information was used to obtain basic drop statistics. Drop diameter was obtained as the arithmetic mean of the diameters obtained from double-pulsed drops.

Basic statistics for drop diameter, velocity and angle

Following image processing, a statistic analysis was performed on the drop data set to obtain centrality and dispersion parameters such as the arithmetic mean, the standard deviation and the coefficient of variation (Eqs. 2, 3 and 4, respectively). Two additional centrality parameters were determined for drop diameter: the volumetric mean (D_v) (Eq. 5) and average volumetric diameter (D_{50}). To obtain this parameter, a given set of drops is ordered by diameter and D_{50} is the diameter corresponding to 50 % of the total cumulative volume.

$$\bar{x} = \frac{\sum_{i=1}^{n} x_i}{n} \tag{2}$$

$$\mathrm{SD} = \sqrt{\frac{\sum_{i=1}^{n} (x_i - \bar{x})}{n-1}} \tag{3}$$

$$\mathrm{CV} = \frac{\mathrm{SD}}{\bar{x}} \tag{4}$$

$$D_V = \frac{\sum_{i=1}^{n} d_i^4}{\sum_{i=1}^{n} d_i^3} \tag{5}$$

In the equations above, x represents the analyzed variable (diameter, velocity or angle), n is the total number of drops in the set, and d is drop diameter (mm).

Velocity fields

Equation 1 was used in PTV-SED to determine the module of the velocity vectors, and then to build velocity fields from drops falling at each observation point. The direction of the velocity vectors was also determined from the movement of the centroid of each double-pulsed drop. The software traced a line between both centroids, and drop angle was determined from the horizontal (u) and vertical (v) velocity components (Eq. 1):

$$\theta = \tan^{-1}\left(\frac{u}{v}\right) \tag{6}$$

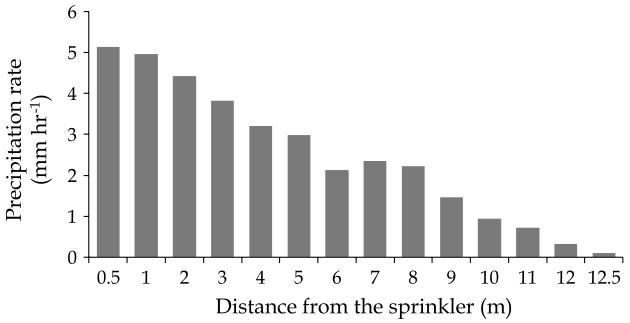

Fig. 4 Radial application pattern for a WR-33 sprinkler equipped with two nozzles of 3.2 and 4.37 mm, and operating at a pressure of 175 kPa

Results and discussion

Radial application pattern

Figure 4 presents the radial application pattern corresponding to the WR-33 impact sprinkler operating at 175 kPa. The Figure shows that the maxim value of precipitation rate was obtained at a horizontal distance from the sprinkler of 0.50 m, with 5.13 mm h^{-1}. The precipitation rate decreased with distance, but showed a local maximum at 7.0 m from the sprinkler. Precipitation continued decreasing to reach the minimum value of 0.1 mm h^{-1} at a distance of 12.5 m. The average precipitation along the irrigated radius was 2.48 mm h^{-1}.

Validation of PTV drop diameter measurements

The 25.0 μm polyamide particles resulted in PTV measurements ranging between 24.18 and 26.4 μm, with average of 25.4 μm. In the case of 50.0 μm particles, the minimum and maximum PTV detected values were 49.2 and 52.5 μm, respectively, with an average of 50.91 μm. The resulting average overestimation error of PTV measurements was 1.48 and 1.82 % for particle diameters of 25.0 and 50.0 μm, respectively.

In the experiment based on metallic spheres, the extreme PTV measurements were as follows: 3.71 and 3.98 for 3.80 mm spheres, with an average of 3.87 mm; 3.90 and 4.33 for 4.20 mm spheres, with an average of 4.25 mm; and 6.30 and 6.55 for 6.42 mm spheres, with an average of 6.53 mm. The resulting average overestimation error of PTV measurements was 1.84, 1.19 and 1.71 % for particle diameters of 3.80, 4.20 and 6.42 mm, respectively.

The moderate diameter overestimations resulting from the PTV technique seem to be related to camera resolution and to the distance between the camera and the target. Salvador et al. (2009) reported a smaller average error (−0.45 %) when using their low-speed photography method. The larger average errors of the PTV method can be compensated by its capacity for automatic data gathering and analysis. Drop velocity and angle measurements were not explicitly compared to experimental values since they are directly related to the error incurred in the estimation of drop diameter.

Drop characterization: experimental procedures

A number of photographs (2,360 images) were captured for this analysis. Only 37.5 % of them (884 images) contained drops ready to be processed by the PTV algorithm. The rest of images were rejected because they were did not contain drops or contained unfocused drops. After processing, a total of 3,782 drops were obtained. The algorithm controlling differences in drop diameter among pulses rejected about half of the drops, leaving 1,893 valid drops. The low-speed photography technique proposed by Salvador et al. (2009) could use 30 % of the photographs, which contained 1,464 valid drops. In this comparison, it is important to note that the PTV technique reduced by 98 % the time requirements of the technique proposed by Salvador et al. (2009) (4–7 min per drop). PTV analysis automation resulted in a requirement of 4.7 s per drop.

Table 1 presents basic drop characterization statistics for each distance to the sprinkler. As expected, drop diameter increased with distance. This increase can be clearly observed for D_v and D_{50}. The arithmetic drop diameter does not reveal this trend, since it assigns the same averaging weight to drops of different diameter. This is a risky assumption since measured drop diameter fluctuated from 0.27 to 6.59 mm. The standard deviation of drop diameter also increased with distance from the sprinkler, and so did the coefficient of variation, which attained its maximum value (127.6 %) at the distal part of the irrigated area. Small drops were detected at all four distances, as denoted by the values of D_{min}. However, the maximum observed drop diameter (D_{max}) increased with distance, indicating that large drops travel distances proportional to their diameter. Salvador et al. (2009) and Bautista et al. (2009), in their experiments using the low-speed photographic method, determined minimum diameters of 0.4 and 0.86 mm, respectively. In this work, almost 20 % of the drops identified at all distances from the isolated sprinkler are smaller than the minimum diameter obtained from low-speed photography. This translates into a decrease of drop diameter centrality parameters, such as the arithmetic mean.

Regarding drop velocity, the standard deviation and coefficient of variation increased with distance from the sprinkler. The arithmetic average velocity did not show a clear trend, due to the presence of small drops at all distances. Small drops travel slower than large drops. However, the value of V_{max} shows a clear dependence on

Table 1 Statistical parameters for drop diameter, velocity and angle

Variable	Parameters	Distance from the sprinkler (m)			
		5	7	9	12
Diameter (mm)	$\overline{X}$	0.64	0.59	0.74	0.98
	D_v	0.91	2.76	3.94	4.84
	D_{50}	0.75	2.78	3.33	4.66
	SD	0.20	0.66	0.77	1.25
	CV	31.3	111.9	104.1	127.6
	D_{min}	0.35	0.27	0.27	0.27
	D_{max}	1.76	3.60	6.00	6.59
Velocity (m s^{-1})	$\overline{X}$	1.61	0.87	1.44	1.65
	SD	0.56	0.89	0.99	1.17
	CV	34.78	102.30	68.75	70.91
	V_{min}	0.60	0.00	0.01	0.00
	V_{max}	3.90	5.10	5.50	6.06
Angle (°)	$\overline{X}$	36.55	44.36	23.44	15.60
	SD	23.57	25.87	23.46	15.80
	CV	64.5	58.3	100.1	101.3
	A_{min}	0.00	3.47	0.00	0.86
	A_{max}	89.68	89.36	89.82	89.30

Results were obtained from four different distances (5, 7, 9 and 12 m) from the impact sprinkler and at an operating pressure of 175 kPa

$\overline{X}$ = Arithmetic mean

D_v = Volumetric diameter

D_{50} = Diameter corresponding to 50 % of the total cumulative volume

SD = Standard deviation

CV = Coefficient of variation

D_{min} = Minimum observed drop diameter

D_{max} = Maximum observed drop diameter

V_{min} = Minimum drop velocity

V_{max} = Maximum drop velocity

A_{min} = Minimum drop angle

A_{max} = Maximum drop angle

distance to the sprinkler, steadily increasing from 3.90 to 6.06 m s^{-1}. The standard deviation of velocity increased with distance, reflecting the increased variability resulting from the presence of large, fast drops at the distal part of the irrigated area.

Drop angles presented large variation in their trajectories. Experimental data were in agreement with previous findings by Salvador et al. (2009) with respect to the relationship with distance. In general, average angle respect to the vertical decreased with distance, indicating that at the distal part drops showed very vertical trajectories. The standard variation of drop angle also decreased with distance to the sprinkler. Drops with horizontal trajectories (angle close to 0°) and vertical trajectories (close to 90°) could be observed at all observation points. This is particularly true for small drops (<1 mm). These observations contrast with data reported by Salvador et al. (2009). These differences could be attributed to the fact that Salvador et al. (2009) developed their experiments in windless outdoor conditions.

Distribution of drop diameters

Curves of drop diameter distribution are presented in Fig. 5 for all distances to the sprinkler. The presence of small drops (diameter <1 mm) at all four distances from the sprinkler, and with frequencies often exceeding 80 % can be attributed to the effect of indoor experimental conditions, which prevented evaporation and drift effects. The observation distance with the largest frequency of small drops was 5 m (95.11 %). From this distance onwards, the frequency of small drops decreased as the frequency of large drops increased. The largest drop diameters (>4 mm) were only observed at 9 and 12 m.

In the movement of droplets in the air, inertial forces are more relevant than gravity forces. From this premise, the ballistic theory describes drop motion in the air. The governing equations have been presented by authors such as Carrión et al. (2001). According to these authors, drop acceleration (in the absence of wind) in horizontal direction (A_X) can be given as:

$$A_X = -\frac{3}{4}\frac{\rho_a}{\rho_w}\frac{C_d}{d}V_x \tag{7}$$

where ρ_a is the air density; ρ_w refers to water density; C_d is drag coefficient; drop diameter is d; and V_X corresponds to drop velocity in the x direction.

Regarding the drag coefficient, several authors have proposed experimental equations for its determination. The proposal by Okamura (1968) results in a smaller drag coefficient (C_d) (around 20 %) for a 3 mm drop diameter than for a 0.3 mm drop diameter. In other hand, the application of the methodology proposed by Li and Kawano (1995) to these two drop diameters, results in a smaller C_d (23 %) for the large drop diameter than for the small drop diameter. As a consequence, particles of with a diameter of 0.3 mm undergo larger deceleration (30 %) than particles with a diameter of 3 mm for the same interval of time. For this reason, when large and small drops are emitted by a nozzle, small drops fall at closer distances from the sprinkler than large drops. Several authors (Basahi et al. 1998; Bautista et al. 2009; Bavi et al. 2009; Eigel and Moore 1983; Kincaid et al. 1996; Kohl et al. 1985; Li et al. 1994; Montero et al. 2003; Salvador et al. 2009; Sudheer and Panda 2000) have experimentally confirmed this behavior in sprinkler irrigation systems.

Figure 6 depicts the cumulative drop diameter frequency (Fig. 6a) and the cumulative application volume (Fig. 6b)

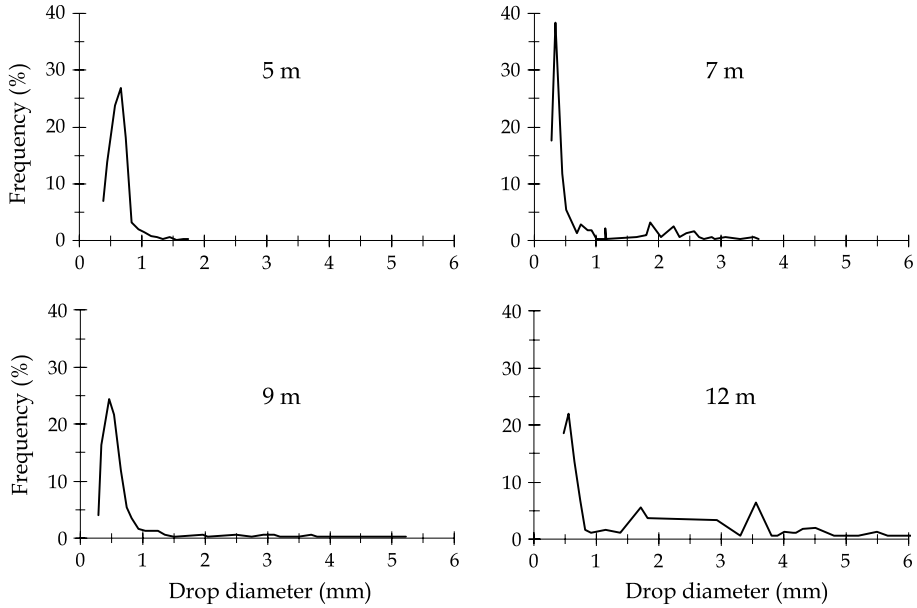

Fig. 5 Curves of drop diameter frequency at the four observations points (distances of 5, 7, 9 and 12 m from the impact sprinkler)

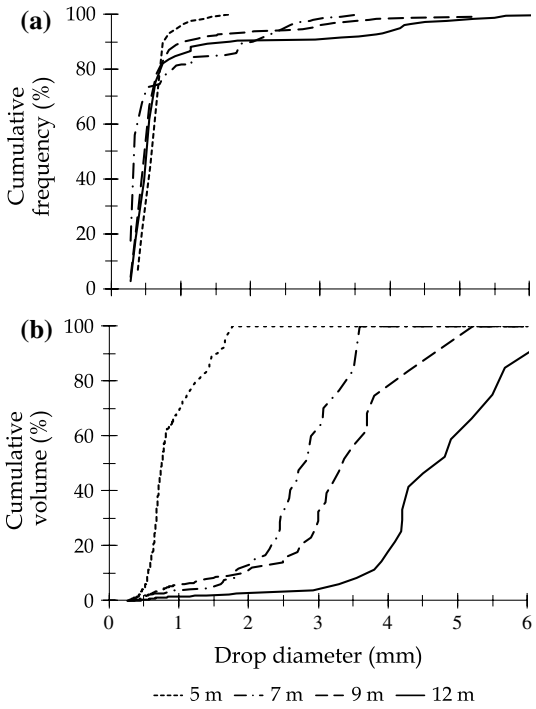

Fig. 6 Cumulative histograms of drop frequency (**a**) and application volume (**b**) at 5, 7, 9 and 12 m from the impact sprinkler

for all four observation points as a function of drop diameter. Cumulative frequency lines approach 100 % at smaller drop diameters than it does for cumulative volume, indicating the relevant volumetric effect of large drops. The largest volume of small drops (<1 mm) occurred at 5 m, with 69.17 %; on the contrary, a very low volume of small drops was found at 12 m (1.37 %). Drop diameters between 2 and 5 mm were not very important in terms of frequency at 7 and 9 m, with an average of 6.67 %. Drop diameters exceeding 5 mm represented 2.26 % at a distance of 12 m, but accounted for 41.38 % of the applied water volume at that distance.

Relationship between drop diameter, velocity and angle

Drop diameter and velocity data were pooled (all observation distances) and presented in a scatter plot (Fig. 7a). Logarithmic models were used to fit the data at each observation distance (Fig. 7b); moreover, a regression curve was obtained by grouping the data series for all analyzed distances. The resulting coefficients of determination (R^2) are presented for all equations. The validity of this regression equation is limited to the experimental range of diameters and distances.

Regarding drop angle (θ), a scatter plot is presented in Fig. 8 for all distances from the sprinkler. Large amplitude in drop angle could be appreciated (from 1° to 90°). This is particularly true for small diameters (<1 mm), owing to the erratic trajectories often exhibited by these very fine drops. Salvador et al. (2009) reported experimental results obtained at 200 kPa, with angles ranging between 40° and 90°. Bautista et al. (2009), using the same low-speed photographic technique in indoor experiments, reported angles of 65° to 90° at the same pressure. Differences between the results reported by those authors and the results reported in this paper can be largely attributed to the vertical distance between the nozzle sprinkler and the camera: 1.35 m for Salvador et al. (2009); 0.50 m for Bautista et al. (2009) and 0.15 m in this work.

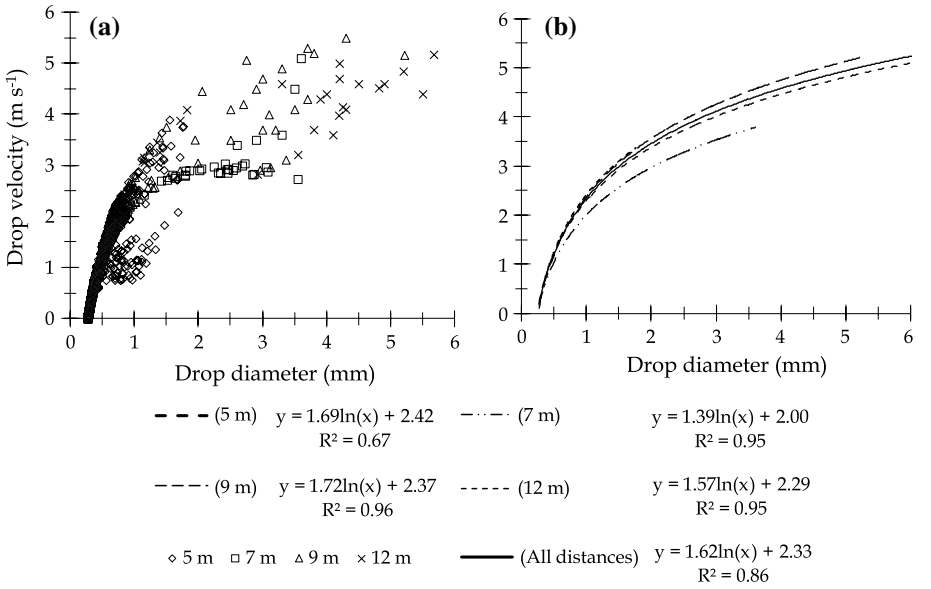

Fig. 7 Relationship between drop diameter and drop velocity. **a** Scatter plot for of all observation distances, represented with different symbols. **b** Regression curves, equations and coefficients of determination (R^2) are presented for each distance from the sprinkler

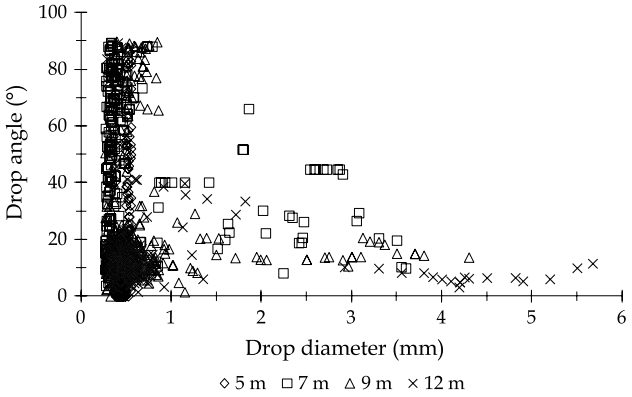

Fig. 8 Relationship between drop diameter and drop angle. Each observation distance is represented with a *different symbol*

Velocity fields

Velocity fields are depicted in Fig. 9 for all observation distances from the sprinkler. Vectors are displayed inside the capture region of the camera (6 by 5 cm). A sample of 100 vectors has been represented in each observation point. Each of these represents the velocity module and direction of flow resulting from the analysis of double-pulsed drops. A velocity scale (valid for all four velocity fields) and the drop trajectory from the sprinkler are included in the figure for clarity. Velocity fields obtained at distances of 5 and 7 m are mostly populated by small drops (usually <1 mm) with low velocities (between 0.6 and 2.5 m s^{-1}). This contrasts with the situation at distances 9 and 12 m, where large drops with velocities ranging 2.28–6.06 m s^{-1} are present.

Conclusions

This paper presents a novel application of the PTV technique to measure the diameter, velocity and angle of drops emitted by an isolated agricultural impact sprinkler in indoor conditions. In the experimental conditions, the overall average drop diameter was 0.80 mm; the volumetric diameter ranged from 0.91 mm at 5 m to 4.84 mm at 12 m. Drop velocity ranged between an absolute minimum of 0.60 m s^{-1} to an absolute maximum of 6.06 m s^{-1}. Although the angle is not a central variable in drop characterization, it can be used to address a number of pending issues in ballistic model formulation. The average drop angle was 30°, ranging between an average of 36.55° at a distance of 5 m and an average of 15.60° at a distance of 12 m. A regression equation was presented for the estimation of drop velocity from drop diameter ($R^2 = 0.956$).

The PTV error in diameter measurement resulted larger than for the low-speed photography technique. However, the value of this error depends on camera settings and camera resolution. In the experimental conditions, the PTV technique permitted to identify very small drops (>0.27 mm). This contrasts with techniques proposed by Sudheer and Panda (2000) (Digital technique), Montero

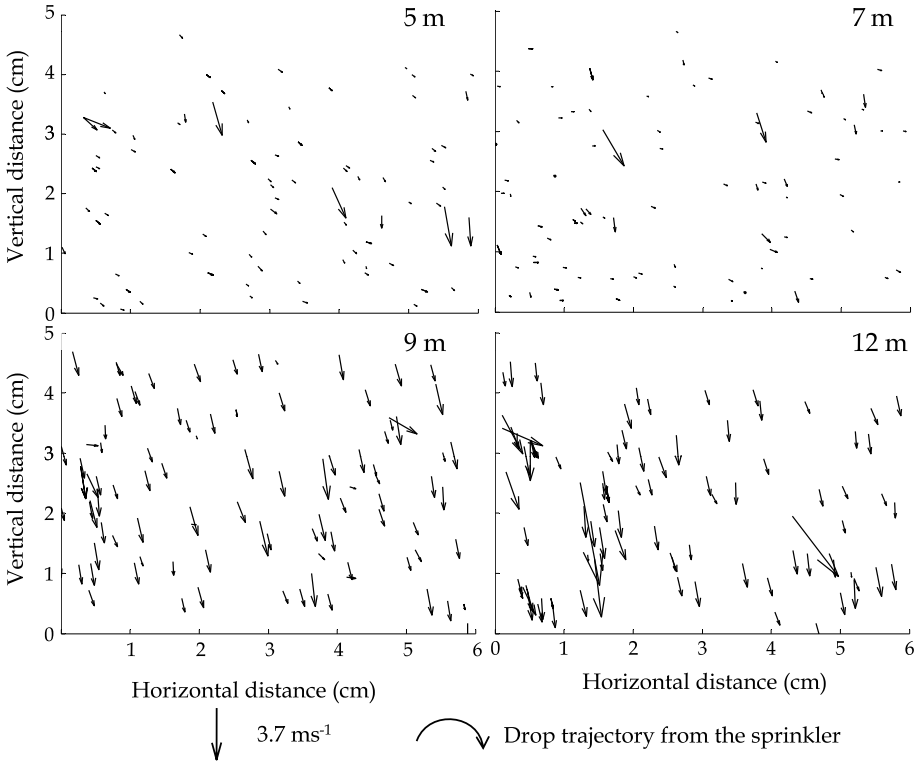

Fig. 9 Velocity fields of the drops emitted by impact sprinkler at four distances from the sprinkler (5, 7, 9 and 12 m). A hundred vectors are represented at each *plot*. A velocity scale and an indication of the drop trajectory are included at the *lower part* of the figure

et al. (2003) (optical spectropluviometer) or Salvador et al. (2009) (photographic technique), where the minimum diameter was about 0.4 mm. A small detection threshold for drop diameter can be useful to assess drift losses in outdoor experiments. Much lower detection thresholds could be obtained by the PTV technique, as demonstrated through the calibration experiment using 25.0 and 50.0 μm particles.

The proposed technique can overcome some of the limitations reported for previously used techniques, such as skillful operation, time-consuming processing or experimental difficulties. The PTV technique is characterized by semi-automatic operation and fast image processing. The use of specific software not only permits automation, but also avoids manual measurement or perception errors. Nevertheless, PTV is a very expensive technique, owing to the required optical equipment, which needs to be adequately waterproof. The use of a laser light source requires the experimental space to be completely in the dark in order to guarantee the correct visibility of drops in the images. This requirement often derives in night operation.

Information is provided in this paper which can lead to the refinement of the PTV technique for its application to agricultural impact sprinklers. Further research should concentrate on specific comparisons with other measurement techniques and on the analysis of wind effects on sprinkler irrigation. In this case, the use of the proposed technique in outdoor conditions will be an additional challenge.

Acknowledgments Thanks are due to the Centro Interamericano de Recursos del Agua from the Universidad Autónoma del Estado de México and to the Maestría en Ingeniería Aplicada Orientación Recursos Hidráulicos of Universidad Autónoma de Zacatecas. Thanks are also due to CONACYT for providing a scholarship to Cruz Octavio Robles Rovelo to pursue Master Degree studies. This research uses the concept of first-last author emphasis.

References

Adrian RJ (1991) Particle imaging techniques for experimental fluid mechanics. Annu Rev Inc Fluid Mech 23:261–304

Anonymous (2004) Agricultural irrigation equipment—Sprinklers Part 3: Characterization of distribution and test methods. ISO 15886-3/2004. International Organization for Standardization. Geneva, Switzerland p. 15

Basahi JM, Fipps G, McFarland MJ (1998) Measuring droplet impact energy with piezoelectric film. J Irrig Drain Eng 124(4):213–217

Bautista C, Salvador R, Burguete J, Montero J, Tarjuelo J, Zapata N, González J, Playán E (2009) Comparing methodologies for the characterization of water drops emitted by an irrigation sprinkler. Trans ASABE 52(5):1493–1504

Bautista C, Zavala M, Playán E (2012) Kinetic energy in sprinkler irrigation: different sources of drop diameter and velocity. Irrig Sci 30(1):29–41

Bavi A, Kashkuli HA, Boroomand S, Naser A, Albaji M (2009) Evaporation losses from sprinkler irrigation systems under various operating conditions. J Appl Sci 9(3):597–600

Beard KV (1976) Terminal velocity and shape of cloud and precipitation drops aloft. J Atmos Sci 33:851–864

Carrión P, Tarjuelo JM, Montero J (2001) SIRIAS: a simulation model for sprinkler irrigation: I Description of the model. Irrig Sci 20(2):73–84

Eigel JD, Moore ID (1983) A simplified technique for measuring raindrop size and distribution. Trans ASAE 26(4):1079–1084
Fukui Y, Nakanishi K, Okamura S (1980) Computer evaluation of sprinkler irrigation uniformity. Irrig Sci 2:23–32
Hauser D, Amayenc P, Nutten B, Waldteufel P (1984) A new optical instrument for simultaneous measurement of raindrop diameter and fall speed distributions. J Atmos Ocean Technol 1(3):256–269
Jadhav DB (1985) Raindrop charge and fall velocity measurements at a tropical station. Arch Meteorol Geophys Bioclimatol 33:389–399
Jensen KD (2004) Flow measurements. J Braz Soc Mech Sci Eng 26:400–419
Jones DMA (1956) Rainfall drop-size. Distribution and radar reflectivity, p 20
Kincaid DC (1996) Spraydrop kinetic energy from irrigation sprinklers. Trans ASAE 39(3):847–853
Kincaid DC, Solomon KH, Oliphant JC (1996) Drop size distributions for irrigation sprinklers. Trans ASAE 39(3):839–845
Kohl RA (1974) Drop size distribution from medium-sized agricultural sprinklers. Trans ASAE 17(4):690–693
Kohl RA, DeBoer DW (1984) Drop size distributions for a low pressure spray type agricultural sprinkler. Trans ASAE 27(6):1836–1840
Kohl RA, DeBoer DW, Evenson PD (1985) Kinetic energy of low pressure spray sprinklers. Trans ASAE 28(5):1526–1529
Kunkel B (1971) Fog drop-size distributions measured with a laser hologram camera. J Appl Meteorol 10:482–486
Li J, Kawano H (1995) Simulating water-drop movement from noncircular sprinkler nozzles. J Irrig Drain Div ASCE 121:152–158
Li J, Kawano H, Yu K (1994) Droplet size distributions from different shaped sprinkler nozzles. Trans ASAE 37(6):1871–1878
Montero J, Tarjuelo JM, Carrión P (2003) Sprinkler droplet size distribution measured with an optical spectropluviometer. Irrig Sci 22:47–56
Okamura S (1968) Theoretical study of sprinkler sprays (part 3) on drop size distributions in sprays. Trans Japanese Soc Irrig Drain and Reclam Eng 26:62–67
Pearson J, Martin G (1957) An evaluation of raindrop sizing and counting techniques. Sci Rep 1:1–17
Prasad AK (2000) Particle image velocimetry. Exp Fluids 79(1):51–60
Salinas TH, García AJ (2011) Fórmula experimental para la velocidad de caída de sedimentos en flujo transversal. Tecnología y Ciencias del Agua, antes Ingeniería Hidráulica en México 2(2):175–182
Salinas TH, García AJ, Moreno HD, Barrientos GB (2006) Particle tracking velocimetry (PTV) algorithm for non-uniform and non-spherical particles. Proc Electron Robot Automot Mech Conf CERMA 2:322–327
Salles C, Poesen J, Borselli L (1999) Measurement of simulated drop size distribution with an optical spectro-pluviometer: sample size considerations. Earth Surf Process Landf 24(6):545–556
Salvador R, Bautista-Capetillo C, Burguete J, Zapata N, Playán E (2009) A photographic methodology for drop characterization in agricultural sprinklers. Irrig Sci 27(4):307–317
Sang YL, Yu DK (2004) Sizing of spray particles using image processing technique. KSME Int J 18(6):879–894
Seginer I (1965) Tangential velocity of sprinkler drops. Transactions of the ASAE pp 90–93
Sheppard B (1990) Measurement of raindrop size distribution using a small Doppler radar. J Atmos Ocean Technol 7:255–268
Smits AJ, Lim TT (2000) Flow visualization: techniques and examples. Ed Imperial College Press p 396
Sudheer KP, Panda RK (2000) Digital image processing for determining drop sizes from irrigation spray nozzles. Agric Water Manag 45:159–167
Tarjuelo JM, Ortega JF, Montero J, De Juan JA (2000) Modelling evaporation and drift losses in irrigation with medium size impact sprinklers under semi-arid conditions. Agric Water Manag 43:263–284
Thompson AL, James LG (1985) Water droplet impact and its effect on infiltration. Trans ASABE 28(5):1506–1510
Ulbrich C (1983) Natural variations in the analysis form of the raindrop size distribution. J Clim Appl Meteorol 22:1764–1775
Van Dyke M (1982) An album of fluid motion. Ed Parabolic Press, p 176
Wiesner J (1895) Beiträge zur Kentniss der Grösze des tropischen Regens. Akademie der Wissenschaften, Mathematika-Naturwissenschaften Klasse. Sitz Berl Verl 104:1397–1434